

## Research Article

# Laboratory Study of the Displacement Coalbed CH<sub>4</sub> Process and Efficiency of CO<sub>2</sub> and N<sub>2</sub> Injection

Liguo Wang,<sup>1,2</sup> Yuanping Cheng,<sup>1</sup> and Yongkang Wang<sup>1</sup>

<sup>1</sup> National Engineering Research Center for Coal & Gas Control, China University of Mining & Technology, Xuzhou 221116, China

<sup>2</sup> College of Safety Science and Engineering, Henan Polytechnic University, Jiaozuo 454000, China

Correspondence should be addressed to Yuanping Cheng; [ypc620924@gmail.com](mailto:ypc620924@gmail.com)

Received 9 October 2013; Accepted 11 December 2013; Published 6 March 2014

Academic Editors: A. Durmus and D. Vamvuka

Copyright © 2014 Liguo Wang et al. This is an open access article distributed under the Creative Commons Attribution License, which permits unrestricted use, distribution, and reproduction in any medium, provided the original work is properly cited.

ECBM displacement experiments are a direct way to observe the gas displacement process and efficiency by inspecting the produced gas composition and flow rate. We conducted two sets of ECBM experiments by injecting N<sub>2</sub> and CO<sub>2</sub> through four large parallel specimens (300 × 50 × 50 mm coal briquette). N<sub>2</sub> or CO<sub>2</sub> is injected at pressures of 1.5, 1.8, and 2.2 MPa and various crustal stresses. The changes in pressure along the briquette and the concentration of the gas mixture flowing out of the briquette were analyzed. Gas injection significantly enhances CBM recovery. Experimental recoveries of the original extant gas are in excess of 90% for all cases. The results show that the N<sub>2</sub> breakthrough occurs earlier than the CO<sub>2</sub> breakthrough. The breakthrough time of N<sub>2</sub> is approximately 0.5 displaced volumes. Carbon dioxide, however, breaks through at approximately 2 displaced volumes. Coal can adsorb CO<sub>2</sub>, which results in a slower breakthrough time. In addition, ground stress significantly influences the displacement effect of the gas injection.

## 1. Introduction

The warming of the climate system can very likely be attributed to the increase of greenhouse gases in the atmosphere, from 278 ppm before the industrial revolution to 396 ppm in 2013 [1]. Many nations have begun active measures to decrease CO<sub>2</sub> emissions. There are several methods that can be used to achieve this goal, namely, reducing energy consumption at the production level through more efficient technologies and at the consumption level through changes in lifestyle by extending the use of zero-CO<sub>2</sub> emission technologies such as renewable energies and nuclear energy and by capturing the CO<sub>2</sub> produced and storing it deep underground, separated from the atmosphere. Geological disposal is regarded as a feasible and effective approach to sequester CO<sub>2</sub>, and depleted hydrocarbon reservoirs, deep unminable coal, saline aquifers, and the deep ocean appear to be suitable sites for permanent CO<sub>2</sub> storage [2–4]. Because of the enhanced gas recovery possibilities, coalbeds are one of the most attractive options of all the underground CO<sub>2</sub> storage possibilities because of the dual benefits of CO<sub>2</sub>

storage and the recovery of coalbed methane (CBM). The revenue of methane production can offset the costs of capture, compression, transportation, and storage of CO<sub>2</sub> [5].

Conventional primary recovery of methane, which is performed by pumping out water and depressurizing the reservoir, allows the recovery of 20–60% of the methane originally present in the reservoir [6, 7]. This process is called enhanced coalbed methane recovery (ECBM), which is a technique that is under investigation as a possible approach for the geological storage of CO<sub>2</sub> in the capture and storage system. ECBM recovery is not yet a mature technology in spite of the growing number of pilot and field tests worldwide that have shown its potential and highlighted the attendant difficulties [8–11].

Currently, during ECBM, high-pressure gas goes through hundreds of meters or even kilometers into the coal seam from the wells. It is then discharged from the other wells, which form a complex network. The flooding by injected gas and displacement flows in the coal seam become quite complex. Real-time monitoring of the flow rate and pressure parameters is difficult. Therefore, scholars use physical simulations to study ECBM technology.

ECBM core flooding experiments are a direct way to observe the gas displacement process and efficiency by inspecting the produced gas composition and flow rate. These experiments involve placing a coal sample in a pressure cell and establishing an initial methane content by holding a methane pressure until the adsorption has equilibrated. Gas, for example,  $\text{CO}_2$ , is then injected at one end of the sample, and outflow is allowed to occur at the opposite end via a back-pressure regulator. Monitoring gas rates and composition provides information on the enhanced gas drainage process.

Experimental research in the aforementioned field has been carried out since the early 1980s. Fulton et al. and Reznik et al. conducted  $\text{CO}_2$  floods of both dry- and water-saturated coal cores that were initially saturated with methane. The results indicated that  $\text{CO}_2$  injection can effectively displace the methane [12, 13]. Parakh presented a systematic approach to performing one-dimensional slim tube displacement for enhanced coalbed methane recovery [14]. Displacement experiments with pure  $\text{N}_2$ ,  $\text{CO}_2$ , and various mixtures were presented. The experiments analyzed the influence of injection pressure and injection rate on the methane recovery and evaluated the influence of water on the  $\text{CH}_4$ - $\text{CO}_2$  exchange process [15]. Jessen et al. conducted displacement experiments with pure  $\text{CO}_2$ ,  $\text{N}_2$ , and various mixtures using a coal briquette in which coal particles were formed into a coalpack by pressing ground coal into cylindrical shapes [16]. Connell et al. reported a study of core floods at two pore pressures, 2 MPa and 10 MPa, and used either nitrogen or flue gas (90% nitrogen and 10%  $\text{CO}_2$ ) flooding of core samples initially saturated with methane [17]. Dutka et al. presented a study of  $\text{CO}_2/\text{CH}_4$  exchange sorption in a coal briquette. A briquette with a porosity of 8.3%, a diameter of 0.096 m, and a length of 0.280 m was used. It was observed that a pore pressure depression moving along the briquette accompanies the exchange sorption [18, 19]. Zhou et al. conducted a laboratory and numerical simulation of ECBM with pure  $\text{N}_2$  or  $\text{CO}_2$  as injectants. The results showed that the  $\text{N}_2$  breakthrough occurs earlier than  $\text{CO}_2$  breakthrough [20].

At present, physical simulations mainly focus on competitive adsorption tests with fine-grained coal particles or coalpacks with dimensions measured in millimeters or less, or displacement experiments using loose coal (permeability greater than  $10 \times 10^{-15} \text{ m}^2$ ) and small coal cores, none of which accurately reflects the displacement mechanism and process [12–16].

Therefore, we conducted injection and recovery experiments in the laboratory on large specimens to simulate scenarios of  $\text{CO}_2$  injection and  $\text{CH}_4$  recovery in a coalbed. Coal briquettes of  $300 \times 50 \times 50 \text{ mm}$  were carefully prepared. The change of the pore pressure in the process of displacement, gas composition, and concentration was dynamically monitored. The experiments were conducted to research the influence of injection pressure and crustal stress on methane recovery.

## 2. Experimental Methodology

**2.1. Experimental Principle.** The results of the ECBM process are a combination of the effects of adsorption-desorption,

diffusion, convection, and convective dispersion. Adsorption/desorption of a gas can cause swelling/shrinkage of the coal matrix, influencing the permeability, which makes the displacement process more complex as it is coupled with the stress. This means that the real displacement process cannot be simulated in the laboratory. Physical experiments using large coal samples are expensive and time consuming. To demonstrate the dynamic flooding process, a two-dimensional flooding experimental system under stress conditions was constructed here. The experimental schematic diagram is shown in Figure 1.

**2.2. Experimental Apparatus.** Figure 3 shows a schematic representation of the experimental apparatus used in ECBM tests. The apparatus has seven parts as follows: briquette holder, mechanical loading system, injection system, vacuum-pumping system, gas-sampling system, gas-measuring system, and gas-composition analysis system.

(1) *Briquette Holder.* The enclosure walls of the briquette holder are Q235 40 mm thick steel plate. The floor is made of 30 mm thick Q235 steel plate. The cover plate is an activity, which is used for vertical stress loading during the experiment. The experimental cavity size of the cabinet is  $300 \times 70 \times 70 \text{ mm}$ . The briquette holder can withstand gas pressure of 6 MPa, which meets the requirements of the experimental pressure.

(2) *Mechanical Loading System.* During the experiment, the vertical load stress is provided by the press machine. It is considered formation pressure. The range of the press is 0–238 MPa.

(3) *Injection System.* The gas injection system consists of cylinders, a compression system, control valves, and pipeline. The control valves are the main valve and pressure-relief valve (pressure ranges from 0 MPa to 16 MPa). The main valve displays the tank pressure. The pressure-relief valve is used to control injection pressure. The maximum output pressure can be up to 10 MPa.

(4) *Vacuum-Pumping System.* The vacuum-pumping system mainly consists of a JZJX30-4 Roots vacuum pump. Coal can be evacuated to a vacuum of  $<10^{-5} \text{ MPa}$ . After checking the tightness of the connections of the displacement apparatus with the Roots vacuum pump, the degassing gas system is connected by turning off the vacuum pump's air communication valve. The degassing time was not less than 48 h. At the end of the degassing process, the vacuum pump was stopped, so it ceased to communicate with the atmosphere.

(5) *Constant Temperature System.* The briquette holder was placed in a water bath that controlled the experimental temperature, maintaining a constant temperature throughout the experiment. The temperature of this experiment was 303 K.

(6) *Gas-Measuring System.* The gas-measuring system measures the injection and effluent gases. The range is 20–200 mL/min. An optical LXI-B7-type flow meter and

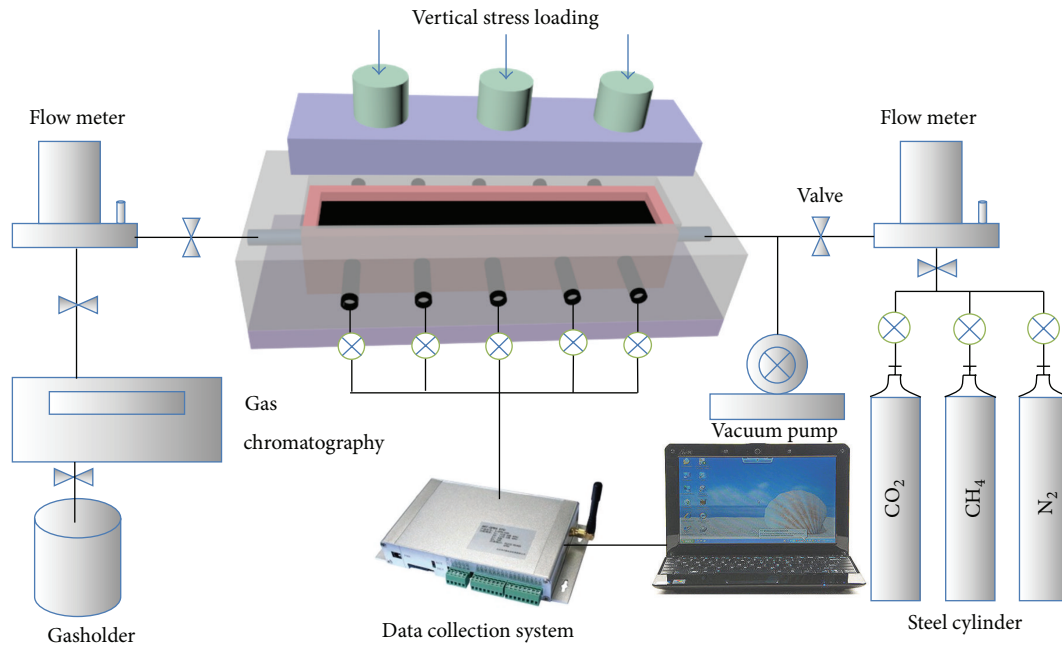


FIGURE 1: Schematic diagram of experimental setup.

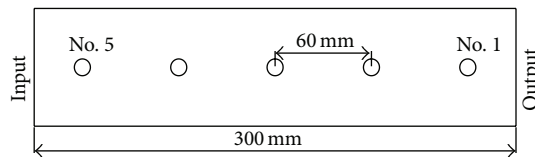


FIGURE 2: Map of measuring pressure and sampling point.

magnetic levitation LXI-B-type measured the effluent gas. The range of the LXI-B7 is 100~1000 mL/min, and the range of the LXI-B is 10~100 mL/min. Each flow meter was equipped with data acquisition software, so a computer can collect the instantaneous flow rate and total flow at different time intervals.

(7) *Gas-Sampling System.* The briquette holder contained six gas sampling points. The distances of the sampling points no. 1–no. 5 from the output of the briquette (no. 0) were as follows: 30 mm, 90 mm, 150 mm, 210 mm, and 270 mm, which are shown in Figure 2. Every sampling point included a 3-way valve that connected to a foil bag used to collect the gas. The arrangement of the manometers is the same as that of the sampling points.

(8) *Gas-Composition Analysis System.* Gas composition was measured with a GC-4000A gas chromatograph. The effluent gas from the flow meter was then sent to a gas analyzer to determine the fraction of each gas species in the effluent mixture.

2.3. *Experimental Procedures.* (1) Place the coal sample into the briquette holder and set the bath temperature to 25°C.

(2) *Vacuums of the sample:* the displacement device is connected to the vacuum pump. Due to the large experimental cavity space, the vacuuming time is not less than 48 h.

(3) *Injection of methane:* after purging the tube, methane is injected at the desired injection pressure for the experiment, with one end of the experimental setup closed. The flow meter is used to determine the amount of methane injected. Injection should be continued for at least 24–48 hours even if the system has stabilized. This is done to make sure that methane not only remains in a free state but also is adsorbed on the surface of the coal.

(4) *Injection of carbon dioxide:* once the setup is completed, the gas cylinder is turned on, and the injection pressure is adjusted automatically depending on the reducing valve. In general, the injection pressure is more than the original balance pressure of coal specimens.

(5) *Measurements:* the following parameters are recorded during the injection period for the analysis and interpretation of results:

- (i) the mass of CO<sub>2</sub> injected into the briquette,
- (ii) the mass of the CO<sub>2</sub>-CH<sub>4</sub> mixture flowing out of the briquette,
- (iii) the concentration of the CO<sub>2</sub>-CH<sub>4</sub> mixture flowing out of the briquette,
- (iv) pore pressure changes along the briquette.

(6) *Ending the experiment:* the experiment is terminated when steady-state concentration conditions are achieved, that is, when the outflow concentration and rate are equal to the inflow. The next experiment was carried out repeating steps (1)~(6).

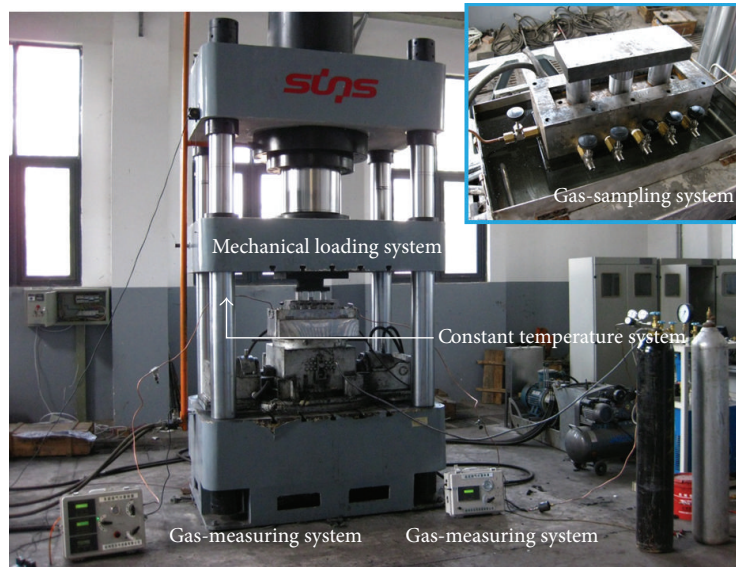


FIGURE 3: Schematic of experimental apparatus for displacement experiments.



FIGURE 4: Physical map of the coal briquette.

**2.4. Sample Description.** The sample used for these experiments was from the Yaojie coalfield in China. The details of the samples are shown in Table 1.

Prior to forming the briquette, the coal material was ground to a granularity of 0.2~0.25 mm. To prevent the gas from directly penetrating through the pore between the experimental enclosure wall and the coal wall to the outlet during the gas displacement process, the inwall of the briquette holder, baseplate, and underside of the bearing plate are coated with 10 mm sealant. After 15 days, the sealant was completely solidified. We put the pulverized coal and a small amount of distilled water into the cavity in the body and artificially compact the pulverized coal. The briquette holder was then placed on the press work surface.

Brown and Hoek summarized the research on the in situ stress measurements by the change rule of vertical stress  $\sigma_v$  with depth  $H$  in various countries as follows [21]:

$$\sigma_v = 0.027H. \quad (1)$$

Based on the fitting formula, we select 14 MPa as vertical stress. The pulverized coal was pressed with a load rate of 1 kN/s to 300 kN, and the force is held at  $300 \pm 5$  kN for 40 minutes. A representative image of the coal briquette is shown in Figure 4.

### 3. Experimental Results

**3.1. Experimental Schemes.** This paper focuses on the displacement coalbed  $\text{CH}_4$  process and efficiency of  $\text{CO}_2$  and  $\text{N}_2$  injection under different gas injection pressures and different stress conditions. The experimental conditions are described in Tables 2 and 3.

#### 3.2. Experimental Results

**3.2.1.  $\text{N}_2$ -ECBM Experiments.** Figure 5 shows the sweep efficiency and concentrations of produced gas against displaced volume with a pressure of 1.5 MPa. Prior to  $\text{N}_2$  injection, 9.7 L of  $\text{CH}_4$  was injected prior to equilibrium. Then,  $\text{N}_2$  injection was carried out. The total volume of injected  $\text{N}_2$  is 31.8 L; the outlet volume of the exhaust gas is 36.04 L, including 9.1 L of  $\text{CH}_4$  and 26.94 L of  $\text{N}_2$ ; 4.86 L of  $\text{N}_2$  is retained in the coal body. It can be seen that  $\text{N}_2$  breaks through at approximately 0.5 displaced volumes.

Sweep efficiency and displaced volume are defined as follows:

$$\text{sweep efficiency (\%)} = \frac{\text{volume of injected displacing gas}}{\text{volume of } \text{CH}_4 \text{ initially in place}},$$

$$\text{displaced volume} = \frac{\text{volume of injected displacing gas}}{\text{volume of } \text{CH}_4 \text{ initially in place}}. \quad (2)$$

Figure 6 shows the sweep efficiency and concentrations of produced gas against displaced volume at 1.8 MPa. The total volume of injected  $\text{N}_2$  is 37.21 L; the outlet volume of the exhaust gas is 41.1 L, including 9.24 L of  $\text{CH}_4$  and 31.86 L of  $\text{N}_2$ ; and 5.35 L of  $\text{N}_2$  is retained in the coal body, which indirectly indicates that  $\text{N}_2$  is more volatile and less strongly adsorbing than methane.  $\text{N}_2$  breaks through at approximately 0.36 displaced volumes.

TABLE 1: Properties of coal sample.

Sample no.	Proximate analysis/%				Maceral/%			$R_0$ /%
	$M_{ad}$	$A_d$	$V_{daf}$	$FC_d$	Vitrinite	Inertinite	Exinite	
No. 1	1.90	7.44	27.4	67.2	60.57	38.18	0	1.09

TABLE 2: Displacement experiment conditions and the results of different pressures of gas injection.

Number	Injectant gas	Injection pressure/MPa	Displaced volume	Sweep efficiency/%
Test 1	N <sub>2</sub>	1.5	0.4	93.8
Test 2	N <sub>2</sub>	1.8	0.5	95.26
Test 3	N <sub>2</sub>	2.2	0.3	97.11
Test 4	CO <sub>2</sub>	1.5	2.4	94.44
Test 5	CO <sub>2</sub>	1.8	2.2	97.14
Test 6	CO <sub>2</sub>	2.2	1.9	98.28

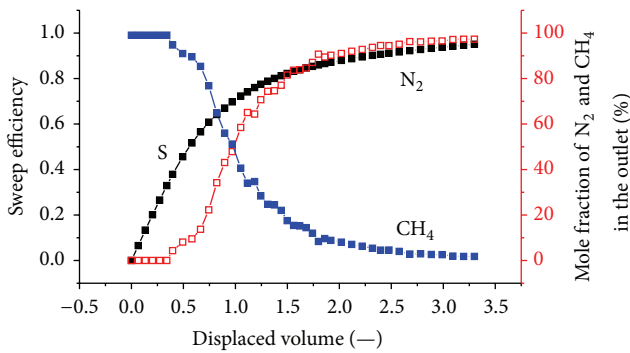


FIGURE 5: The sweep efficiency and concentrations of produced gas against displaced volume at 1.5 MPa.

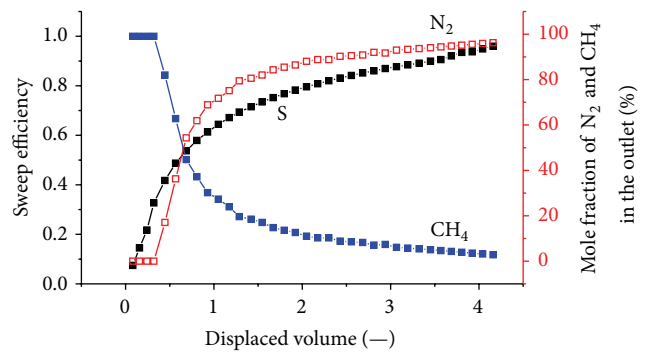


FIGURE 7: The sweep efficiency and concentrations of produced gas against displaced volume at 2.2 MPa.

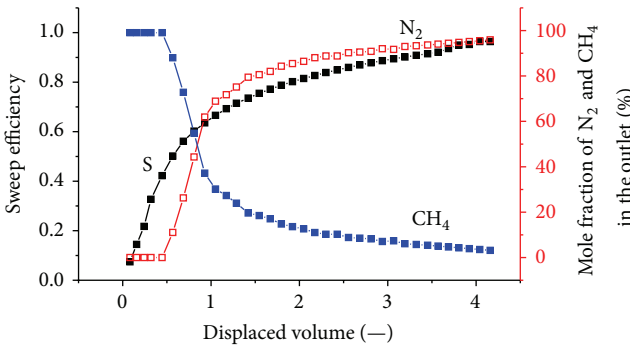


FIGURE 6: The sweep efficiency and concentrations of produced gas against displaced volume at 1.8 MPa.

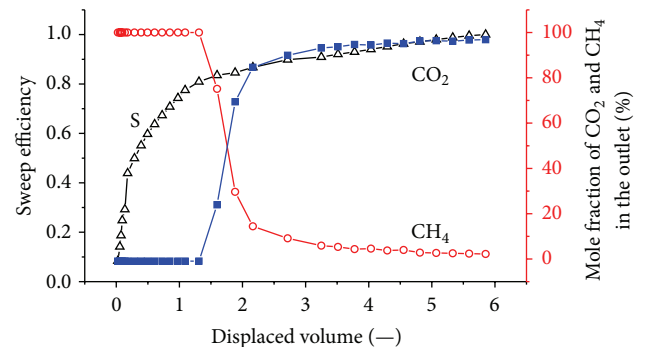


FIGURE 8: The sweep efficiency and concentrations of produced gas against displaced volume with a vertical stress of 14 MPa.

Figure 7 shows the sweep efficiency and concentrations of produced gas against displaced volume at 2.2 MPa. The total volume of injected N<sub>2</sub> is 36.9 L; the outlet of the exhaust gas is 40.18 L, including 9.42 L of CH<sub>4</sub> and 30.76 L of N<sub>2</sub>; and 6.14 L of N<sub>2</sub> is retained in the coal body.

3.2.2. CO<sub>2</sub>-ECBM Experiments under Different Crustal Stresses. Figure 8 shows the sweep efficiency and concentrations of produced gas against displaced volume with a crustal stress of 14 MPa. The injection pressure is 1.5 MPa.

It can be seen that CO<sub>2</sub> breaks through at approximately 1.4 displaced volumes. The total volume of injected CO<sub>2</sub> is 43.91 L; the outlet volume of the exhaust gas is 31.89 L, including 7.5 L of CH<sub>4</sub> and 24.38 L of CO<sub>2</sub>; and there is 19.53 L of CO<sub>2</sub> retained in the coal body. The gross ratio of the CO<sub>2</sub>/CH<sub>4</sub> displacement was approximately 2.6. At this time, the percentage of CH<sub>4</sub> at the output is almost zero, indicating that the CH<sub>4</sub> gas in the coal is completely displaced.

Figure 9 shows the sweep efficiency and concentrations of produced gas against the displaced volume with a crustal

TABLE 3: Displacement experiment conditions and results under different stress conditions.

Number	Stress/MPa	Injectant gas	Injection pressure/MPa	Displaced volume	Sweep efficiency/%
Test 7	14	CO <sub>2</sub>	1.5	1.4	97.82
Test 4	19	CO <sub>2</sub>	1.5	2.4	94.44

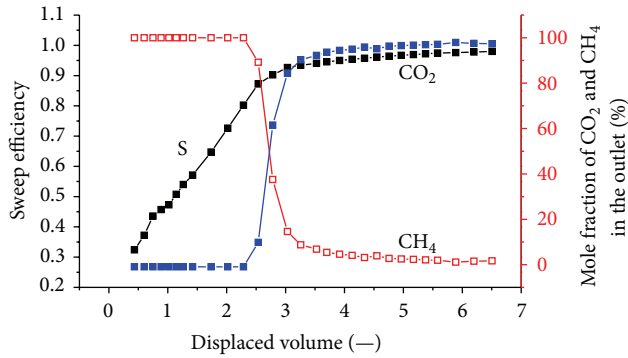


FIGURE 9: The sweep efficiency and concentrations of produced gas against displaced volume at 1.5 MPa.

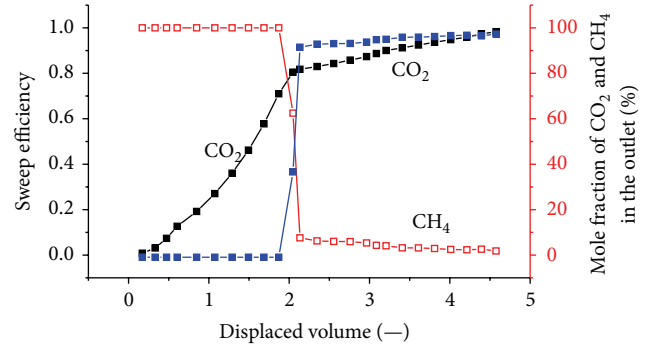


FIGURE 11: The sweep efficiency and concentrations of produced gas against displaced volume at 2.2 MPa.

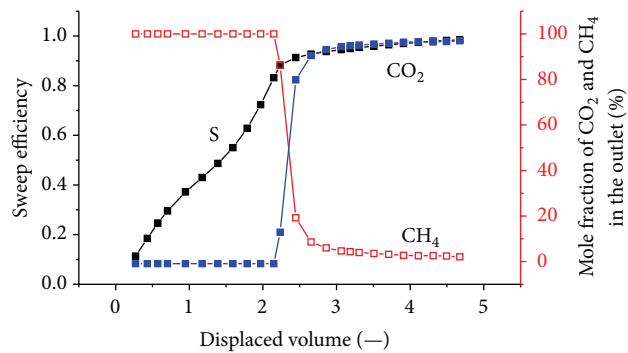


FIGURE 10: The sweep efficiency and concentrations of produced gas against displaced volume at 1.8 MPa.

stress of 19 MPa. The injection pressure is 1.5 MPa. The total volume of injected CO<sub>2</sub> is 44.5 L; the outlet volume of the exhaust gas is 20.91 L, including 8.8 L of CH<sub>4</sub> and 12.11 L of CO<sub>2</sub>; and there is 32.39 L of CO<sub>2</sub> retained in the coal body. The gross ratio of the CO<sub>2</sub>/CH<sub>4</sub> displacement was approximately 3.69.

**3.2.3. CO<sub>2</sub>-ECBM Experiments under Various Injection Pressures.** In Tests 4, 5, and 6 (Table 2), CO<sub>2</sub>-ECBM experiments were carried out. The injection pressure is 1.5 MPa, 1.8 MPa, and 2.2 MPa, respectively, and the crustal stress is 19 MPa. The results are shown in Figures 9, 10, and 11.

Figure 10 shows the sweep efficiency and concentrations of produced gas against displaced volume at 1.8 MPa. Prior to CO<sub>2</sub> injection, 9.8 L of CH<sub>4</sub> was injected to achieve equilibrium. The total volume of injected CO<sub>2</sub> is 44.53 L; the outlet volume of the exhaust gas is 27.73 L, including 9.52 L of CH<sub>4</sub> and 18.21 L of CO<sub>2</sub>; and there is 26.32 L of CO<sub>2</sub> retained in the coal body. CO<sub>2</sub> breaks through at

approximately 2.2 displaced volumes. The gross ratio of the CO<sub>2</sub>/CH<sub>4</sub> displacement was approximately 26.32/9.52 = 2.76.

Figure 11 shows the sweep efficiency and concentrations of produced gas against displaced volume at 2.2 MPa. The total volume of injected CO<sub>2</sub> is 44.72 L; the volume of the exhaust gas is 30.24 L, including 9.73 L of CH<sub>4</sub> and 20.51 L of CO<sub>2</sub>; and there is 24.21 L of CO<sub>2</sub> retained in the coal body. CO<sub>2</sub> breaks through at approximately 1.9 displaced volumes. The gross ratio of the CO<sub>2</sub>/CH<sub>4</sub> displacement was approximately 24.21/9.73 = 2.4.

## 4. Discussion

**4.1. Influence of Gas Species on Displacement Efficiency.** The results show that CO<sub>2</sub> breaks through at approximately 2 displaced volumes. According to mass conservation, for flow in a porous medium, the injection gas should appear at the tube outlet after one pore volume is injected. In this case, as CO<sub>2</sub> is adsorbed on the coal, the volume of CO<sub>2</sub> in the free space is reduced and more than one displaced volume is required to see the breakthrough. It can also be seen that CO<sub>2</sub> breaks through as a sharp front. This is due to the presence of a shock between the injection and the initial tie line.

N<sub>2</sub> is more volatile and less strongly adsorbing than methane, so it travels quickly through the system, causing methane to desorb earlier than when CO<sub>2</sub> is injected. More molecules of methane are desorbed for every molecule of N<sub>2</sub> that is adsorbed. Therefore, volume is added to the flowing gas phase, thereby increasing the flow velocity. The N<sub>2</sub> front is highly dispersed compared to the CO<sub>2</sub> front in Figures 5, 6, and 7. For example, when the N<sub>2</sub> concentration in the output is 3%, the sweep efficiency is 46%. However, when the N<sub>2</sub> concentration increases to 50%, the sweep efficiency is 72%. There is CH<sub>4</sub> in the output after N<sub>2</sub> breaks through for a long time.

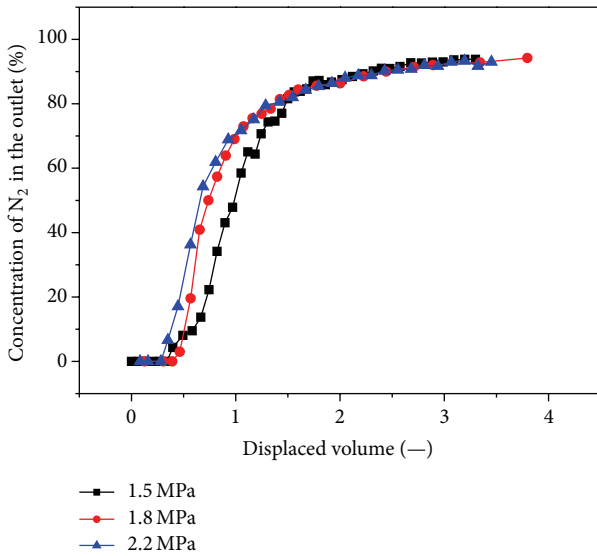


FIGURE 12: Influence on the  $N_2$  concentration by gas injection pressure.

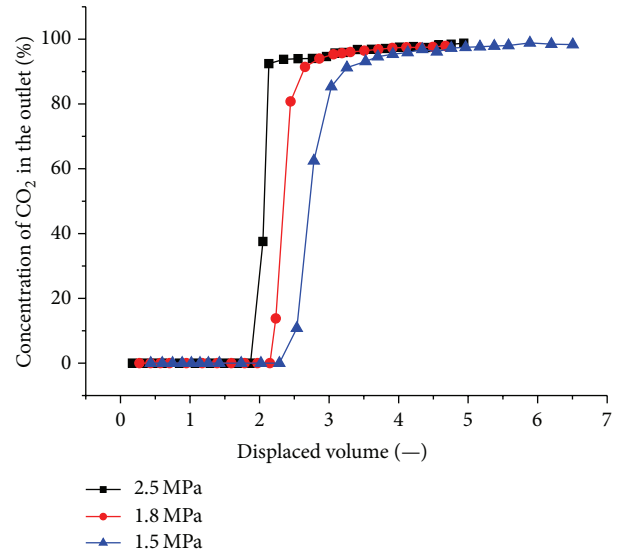


FIGURE 13: Influence on the output  $CO_2$  concentration by different gas injection pressures.

4.2. *Influence of Gas Injection Pressure on Displacement Efficiency.*  $N_2$  is more volatile and less strongly adsorbing than methane, so it travels quickly through the system. With a higher injection pressure, the discharge of the methane volume gradually increases, and the  $N_2$  content in the coal briquette also increases. This occurs because the higher injection pressure further reduces the partial pressure of  $CH_4$  in the coal briquette so more  $CH_4$  is desorbed. We found that the breakthrough time of  $N_2$  decreases gradually with increasing injection pressure, as shown in Figure 12.

$CO_2$  is more adsorbing and less volatile than  $CH_4$ . When  $CO_2$  is injected, it is preferentially adsorbed by coal in comparison to methane. The  $CH_4$  is displaced. With the higher injection pressure, the adsorption of  $CO_2$  onto the coal increases, and more  $CH_4$  is desorbed. Figure 13 shows the  $CO_2$  concentration profile versus the injected volume at the different injection pressures. The breakthrough time of  $CO_2$  was similar in all cases; however, after breakthrough, the produced  $CO_2$  concentration behaved somewhat differently. With high pressure, the effluent concentration increases sharply, indicating that the displacement is piston-like. When the pressure is lower, the produced  $CO_2$  concentration is more dispersed. Higher pressure reduces the time required for  $CO_2$  to displace  $CH_4$  from coal surfaces.

The sampling points along the length of the coal pack allow the measurement of the composition of the free gas during the tests. Figure 14 shows the gas composition of sampling points versus the injected volumes at 1.5 MPa injection pressure. The figure indicates that the closer the distance from the inlet, the steeper the  $CO_2$  concentration changes. We obtain similar curves at other injection pressures.

4.3. *Influence of the Stress on Displacement Efficiency.* When coal exhibits high permeability, the flow rate of  $CO_2$  in the coal is also high. The coal does not adsorb  $CO_2$  sufficiently, so sweeping plays an important role in the displacement process.

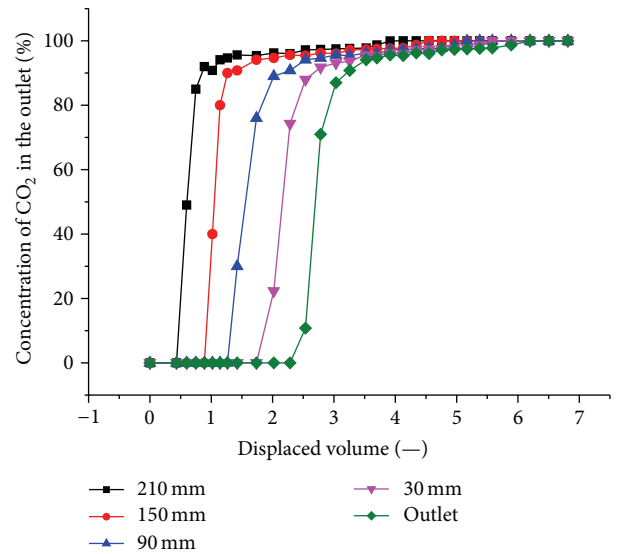


FIGURE 14:  $CO_2$  concentration versus time sampled from various locations along the length of the coal pack. The injection pressure of  $CO_2$  was maintained at 1.5 MPa.

Most of the  $CH_4$  is swept away by  $CO_2$  rather than removed primarily by replacement. Once the permeability decreases, the flow rate of  $CO_2$  in the coal slows.  $CO_2$  can then be adsorbed onto the coal, and  $CH_4$  is flooded out step by step under the effect of  $CO_2$ . Therefore, the  $CO_2$  breakthrough time gradually slowed from 1.4 to 2.4 displaced volumes. After the  $CO_2$  breakthrough at the outlet, the concentration of  $CO_2$  soon reaches 90%.

Mazumder et al. studied raw coal. The change in the gas concentration in the outlet is not in accordance with this experiment [15]. In this study,  $CO_2$  breaks through air outlet, so its concentration does not increase quickly (to more than

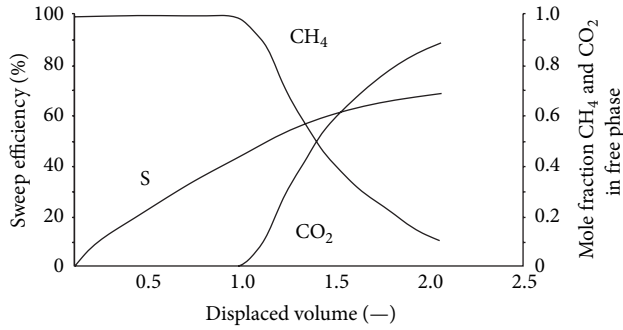


FIGURE 15: The sweep efficiency and molar concentrations of the produced gas against the displaced volume.

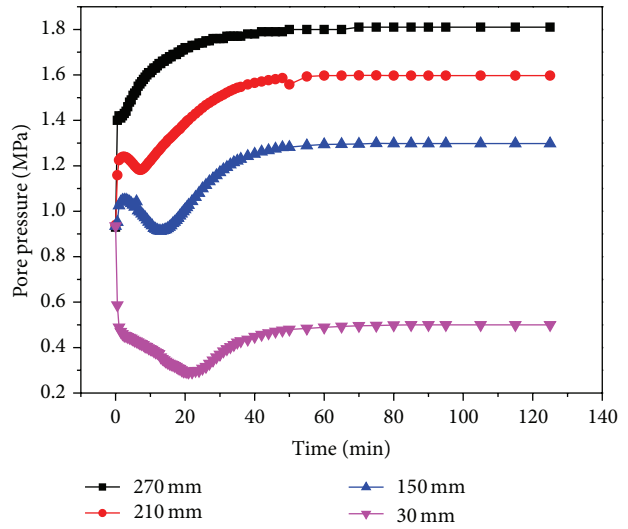


FIGURE 17: The change of pore pressure during CO<sub>2</sub>-ECBM at 1.8 MPa.

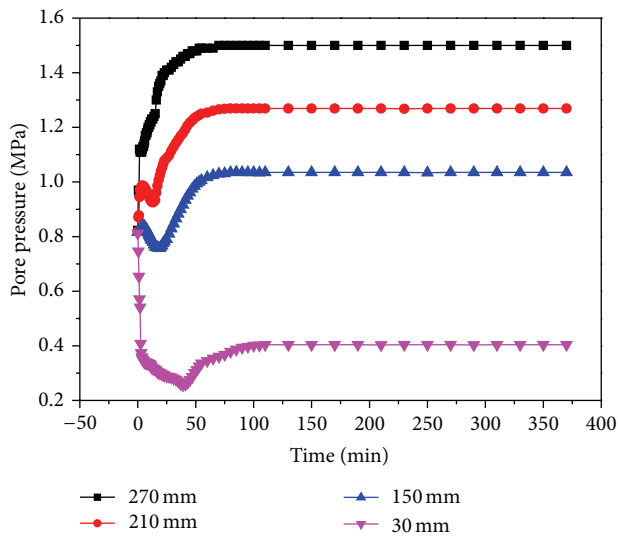


FIGURE 16: The change in pore pressure during CO<sub>2</sub>-ECBM at 1.5 MPa.

90%), as shown in Figure 15. This experiment uses the coal briquette made from 0.20~25 mm size of pulverized coal, so the time for diffusive exchange of gases from the particle exterior to the center of the particle is quite short. CH<sub>4</sub> can quickly be desorbed from the coal matrix. In regard to intact coal, the permeability of coal is low in general. The time required for the diffusion of gas from the outside to the core is slow, leading to a slower CH<sub>4</sub> desorption rate. CH<sub>4</sub> can continue to spread out from a coal matrix. The results of this paper are consistent with those of Parakh [14].

**4.4. Pore Pressure Changes Accompanying the ECBM Experiments.** Figures 16 and 17 show the pore pressure changes accompanying the ECBM experiments with injection pressures of 1.5 MPa and 1.8 MPa under a crustal stress of 19 MPa. The point “30 mm” is close to the outlet, and the pressure drops the fastest here in the early stages. When CO<sub>2</sub> is injected continuously, at this location the pressure is the lowest at 0.26 MPa. The pressure then increases gradually and is stable after 110 minutes. The point “270 mm” is close to the

inlet and is not affected by the exhaust outlet. The pressure increases continuously to a level that is slightly lower than the injection pressure. For the other points “150 mm” and “210 mm”, the pore pressure increases over a short period of time and then reduces and increases until a stable value is finally reached. The other groups of experiments also showed a similar curve.

### 5. Main Conclusions

We have presented experimental results of two ECBM tests carried out using N<sub>2</sub> and CO<sub>2</sub> as injectants. The pressures at the outlet and inlet points, the gas production rate, and gas composition are reported. The main conclusions follow.

Gas injection significantly enhances CBM recovery. The experimental recoveries of the original gas are in excess of 93% for all cases. When 0.5 displaced volumes are injected, N<sub>2</sub> breaks through the outlet. With increasing injection pressure, the breakthrough time shortens. N<sub>2</sub> advances more rapidly and displays a more dispersed front than CO<sub>2</sub>, which is more adsorbing and less volatile than CH<sub>4</sub>. Therefore, CO<sub>2</sub> breakthrough requires the injection of more than one displaced volume. At three injection pressures of 1.5 MPa, 1.8 MPa, 2.2 MPa, CO<sub>2</sub> breaks through at 1.4~2.4 displaced volumes. CO<sub>2</sub> moves through coal in a piston-like fashion. Once CO<sub>2</sub> breaks through the outlet, the CO<sub>2</sub> concentration quickly achieved high values (more than 90%). The breakthrough time of CO<sub>2</sub> is reduced with increasing injection pressure.

With the increase of *in situ* stress, permeability decreases, and the seepage speed of CO<sub>2</sub> slows in coal. The coal can adsorb CO<sub>2</sub>, which results in a slower breakthrough time. Under a ground stress of 14 MPa, CO<sub>2</sub> breaks through at 1.4 displaced volumes, while at 19 MPa, the breakthrough time is approximately 2.4 displaced volumes. The ground stress significantly influences the displacement effect of gas injection.



## Conflict of Interests

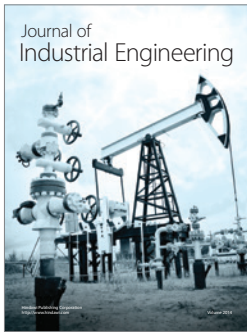
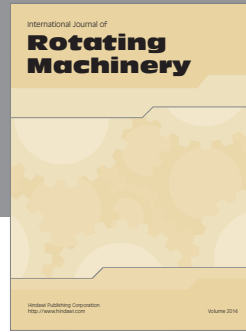
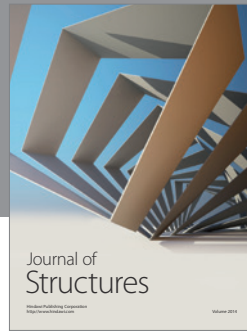
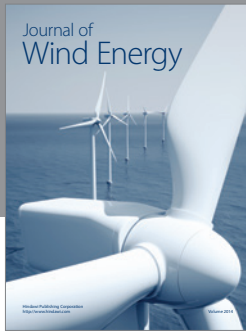
The authors declare that there is no conflict of interests regarding the publication of this paper.

## Acknowledgments

The authors are grateful for the financial support from the National Basic Research Program of China (973 Program, no. 2011CB201204), the National Foundation of China (no. 51074160), and the Natural Science Foundation for the Youth of China (no. 41202118).

## References

- [1] NOAA Earth System Research Laboratory, 2013, <http://www.esrl.noaa.gov/gmd/ccgg/trends/>.
- [2] W. Liang, Y. Zhao, D. Wu, and M. B. Dusseault, "Experiments on methane displacement by carbon dioxide in large coal specimens," *Rock Mechanics and Rock Engineering*, vol. 44, no. 5, pp. 579–589, 2011.
- [3] T. A. Torp and J. Gale, "Demonstrating storage of CO<sub>2</sub> in geological reservoirs: the Sleipner and SACS projects," *Energy*, vol. 29, no. 9-10, pp. 1361–1369, 2004.
- [4] V. T. H. Pham, F. Riis, I. T. Gjeldvik, E. K. Halland, I. M. Tappel, and P. Aagaard, "Assessment of CO<sub>2</sub> injection into the south Utsira-Skade aquifer, the North Sea, Norway," *Energy*, vol. 55, pp. 529–540, 2013.
- [5] K. H. A. A. Wolf, O. Barzandji, W. Bertheux, and J. Bruining, "CO<sub>2</sub>-sequestration in The Netherlands. CO<sub>2</sub>-injection and CH<sub>4</sub>-production as related to the Dutch situation: laboratory experiments and field simulation," in *Proceedings of the 5th International Conference on Greenhouse Gas Control Technologies (GHGT '00)*, Cairns, Australia, 2000.
- [6] S. H. Stevens, D. Spector, and P. Riemer, "Enhanced coalbed methane recovery using CO<sub>2</sub> injection: worldwide resource and CO<sub>2</sub> sequestration potential," in *Proceedings of the 6th International Oil & Gas Conference and Exhibition in China (IOGCEC'98)*, pp. 489–501, November 1998.
- [7] C. M. White, D. H. Smith, K. L. Jones et al., "Sequestration of carbon dioxide in coal with enhanced coalbed methane recovery—a review," *Energy and Fuels*, vol. 19, no. 3, pp. 659–724, 2005.
- [8] S. Wong, D. Law, X. Deng et al., "Enhanced coalbed methane and CO<sub>2</sub> storage in anthracitic coals-Micro-pilot test at South Qinshui, Shanxi, China," *International Journal of Greenhouse Gas Control*, vol. 1, no. 2, pp. 215–222, 2007.
- [9] W. D. Gunter, M. J. Mavor, and J. R. Robinson, "CO<sub>2</sub> storage and enhanced methane production: field testing at Fenn-Big Valley, Alberta, Canada, with application," in *Proceedings of the 7th International Conference on Greenhouse Gas Control Technologies (GHGT '04)*, Vancouver, Canada, September 2004.
- [10] S. Yamaguchi, K. Ohga, M. Fujioka, and S. Muto, "Prospect of CO<sub>2</sub> sequestration in the Ishikara coal field, Japan," in *Proceedings of the 7th International Conference on Greenhouse Gas Control Technologies (GHGT '04)*, Vancouver, Canada, September 2004.
- [11] S. Sharma, P. Cook, T. Berly, and C. Anderson, "Australia's first geosequestration demonstration project-the CO<sub>2</sub> CRC Otway Basin Pilot project," *APPEA Journal*, vol. 47, pp. 257–268, 2007.
- [12] P. F. Fulton, C. A. Parente, B. A. Rogers, N. Shah, and A. A. Reznik, "A laboratory investigation of enhanced recovery of methane from coal by carbon dioxide injection," in *Proceedings of the SPE Unconventional Gas Recovery Symposium*, Pittsburgh, Pa, USA, May 1980.
- [13] A. A. Reznik, P. K. Singh, and W. L. Foley, "An analysis of the effect of CO<sub>2</sub> injection on the recovery of in-situ methane from bituminous coal. An experimental simulation," *Society of Petroleum Engineers Journal*, vol. 24, no. 5, pp. 521–528, 1984.
- [14] S. Parakh, *Experimental investigation of enhanced coalbed methane recovery [M.S. thesis]*, Stanford University, Stanford, Calif, USA, 2007.
- [15] S. Mazumder, K. H. A. A. Wolf, P. Hemert, and A. Busch, "Laboratory experiments on environmental friendly means to improve coalbed methane production by carbon dioxide/flue gas injection," *Transport in Porous Media*, vol. 75, no. 1, pp. 63–92, 2008.
- [16] K. Jessen, G.-Q. Tang, and A. R. Kovscek, "Laboratory and simulation investigation of enhanced coalbed methane recovery by gas injection," *Transport in Porous Media*, vol. 73, no. 2, pp. 141–159, 2008.
- [17] L. D. Connell, R. Sander, Z. Pan, M. Camilleri, and D. Heryanto, "History matching of enhanced coal bed methane laboratory core flood tests," *International Journal of Coal Geology*, vol. 87, no. 2, pp. 128–138, 2011.
- [18] B. Dutka, M. Kudasik, and J. Topolnicki, "Pore pressure changes accompanying exchange sorption of CO<sub>2</sub>/CH<sub>4</sub> in a coal briquette," *Fuel Processing Technology*, vol. 100, pp. 30–34, 2012.
- [19] B. Dutka, M. Kudasik, Z. Pokryszka, N. Skoczylas, J. Topolnicki, and M. Wierzbicki, "Balance of CO<sub>2</sub>/CH<sub>4</sub> exchange sorption in a coal briquette," *Fuel Processing Technology*, vol. 106, pp. 95–101, 2013.
- [20] F.D. Zhou, F. Hussain, and Y. Cinar, "Injecting pure N<sub>2</sub> and CO<sub>2</sub> to coal for enhanced coalbed methane: experimental observations and numerical simulation," *International Journal of Coal Geology*, vol. 116-117, pp. 53–62, 2013.
- [21] E. T. Brown and E. Hoek, "Trends in relationships between measured in-situ stresses and depth," *International Journal of Rock Mechanics and Mining Sciences*, vol. 15, no. 4, pp. 211–215, 1978.



# Hindawi

Submit your manuscripts at  
<http://www.hindawi.com>

